

# Spin–Orbit Torque-Driven Magnetic Switching of Co/Pt-CoFeB Exchange Spring Ferromagnets

Min Song<sup>1</sup>, Shijiang Luo<sup>1</sup><sup>✉</sup>, Xin Li<sup>1</sup><sup>✉</sup>, Shuai Zhang<sup>2</sup>, Qiang Luo<sup>2</sup>, Zhe Guo<sup>2</sup>, Jeongmin Hong<sup>1</sup><sup>✉</sup>, Bin Zhou<sup>1</sup>, Haoshuang Gu<sup>1</sup>, OukJae Lee<sup>3</sup>, and Long You<sup>1</sup><sup>✉</sup>

<sup>1</sup>Faculty of Physics and Electronic Science, Hubei Key Laboratory of Ferro & Piezoelectric Materials and Devices, Hubei University, Wuhan 430062, China

<sup>2</sup>School of Optical and Electronic Information, Huazhong University of Science and Technology, Wuhan 430074, China

<sup>3</sup>Center for Spintronics, Korea Institute of Science and Technology, Seoul 02792, South Korea

We experimentally investigate spin–orbit torque (SOT) switching of a hybrid exchange spring system (ESS) in which a Co/Pt with perpendicular magnetic anisotropy (PMA) is coupled to a CoFeB thin film with an in-plane (IP) magnetic anisotropy (IMA). The magnetization tilt angle from the out-of-plane can be easily tuned by varying the thickness of the IMA layer due to the competition between PMA and IMA layers. We find that the tilt angle is highly tuned from 0° to 90° over a small range of CoFeB thicknesses, from 0 to 1 nm. The tilted films with high thermal stability are promising materials for a zero/low field operating SOT magnetic random access memory (MRAM) or for a bit patterned magnetic recording media. IP current-induced magnetization switching of Co/Pt-CoFeB ESS is also studied, under an IP magnetic field ( $H_{IP}$ ). The current amplitude for the 45° tilt magnetization switching is almost independent of the  $H_{IP}$  ranged from 50 to 1000 Oe. This phenomenon might be due to the presence of the Dzyaloshinskii–Moriya interaction (DMI) and DMI effective field is expected to be less than 50 Oe.

**Index Terms**—Dzyaloshinskii–Moriya interaction (DMI), exchange spring system (ESS), spin–orbit torque (SOT) switching, titling magnetization.

## I. INTRODUCTION

INCREASING attention has been to the perpendicular exchange spring systems (ESS), which is consisted of exchange-coupled hard and soft magnetic layers with, respectively, out-of-plane (OOP) and in-plane (IP) easy magnetization axes. While the magnetically hard film provides good thermal stability, the soft layer provides a path to reduce the current or field for magnetic reversals [1]–[3]. Moreover, ESS can provide tilted magnetic anisotropy [4]. Compared with purely OOP and IP magnetization directions, a tilted magnetization provides additional degrees of freedom to manipulate its static and dynamic states. More importantly, tilted anisotropy materials may be useful for achieving higher density magnetic recording with stronger thermal stability and faster magnetic switching [5]–[7] and zero-field operation of spin torque oscillators (STOs) [8], [9]. You *et al.* [10] have recently shown that the tilted magnetization could be switched by an IP current via spin–orbit torque (SOT) without the need for an external magnetic field. Tilted anisotropies have traditionally been realized using collimated sputtering [11], by depositing multilayers on nanospheres [6], or via precise nanofabrication [10]. In contrast, exchange spring materials with OOP and IP anisotropies provide a wide and tunable range of tilt angles [4], [12]. Utilizing different thicknesses of the OOP and IP layers as well as different OOP–IP coupling strengths, the average tilt angle can be varied with great freedom. Here, we focus

on hybrid anisotropy exchange spring magnets, which couple the strong PMA (Co/Pt) and in-plane magnetic anisotropy (IMA) (CoFeB) via the exchange interaction between them. By taking advantage of the competition between the PMA and IMA in these systems, we can tune the entire magnetization angle. We also investigate the exchange spring magnets that can be switched by SOT induced by IP currents.

## II. EXPERIMENTS

All film stacks were deposited at room temperature on thermally oxidized Si substrates using a magnetron sputtering system at a background pressure of  $2 \times 10^{-8}$  Torr. All series were prepared on 2 nm Ta seed layers which promotes a strong PMA into our Pt (5nm)/Co (1 nm) layer. On top of the PMA layer, a CoFeB layer with various thickness was deposited and covered by a 2 nm MgO capping layer to protect surface oxidation. Another 2 nm Ta layer was deposited on top of the MgO layer. The deposition rates were  $\sim 0.4\text{--}0.5 \text{ \AA/s}$ . Magnetic properties of the thin films were characterized by vibrating sample magnetometer (VSM). Then, the films were patterned into  $2 \mu\text{m} \times 6 \mu\text{m}$  Hall bar structures by an etching process. The electric transport of microscale devices was also studied in a probe station with electromagnet.

## III. RESULTS AND DISCUSSION

We measured the OOP (black curve) and the IP (red curve) hysteresis loop for Ta (2 nm)/Pt (5 nm)/Co (1 nm)/CoFeB ( $t$  nm)/MgO (2 nm)/Ta (2 nm) exchange spring films at room temperature. The CoFeB thickness ( $t_{CoFeB}$ ) varies from 0 to 1 nm. We observed the strong out-of-plane anisotropy(OPA) for the films of Pt/Co layer, as shown

Manuscript received December 20, 2018; revised February 19, 2019; accepted April 11, 2019. Date of publication May 3, 2019; date of current version July 18, 2019. Corresponding author: L. You (e-mail: lyou@hust.edu.cn).

Color versions of one or more of the figures in this paper are available online at <http://ieeexplore.ieee.org>.

Digital Object Identifier 10.1109/TMAG.2019.2911571

0018-9464 © 2019 IEEE. Personal use is permitted, but republication/redistribution requires IEEE permission.  
See [http://www.ieee.org/publications\\_standards/publications/rights/index.html](http://www.ieee.org/publications_standards/publications/rights/index.html) for more information.

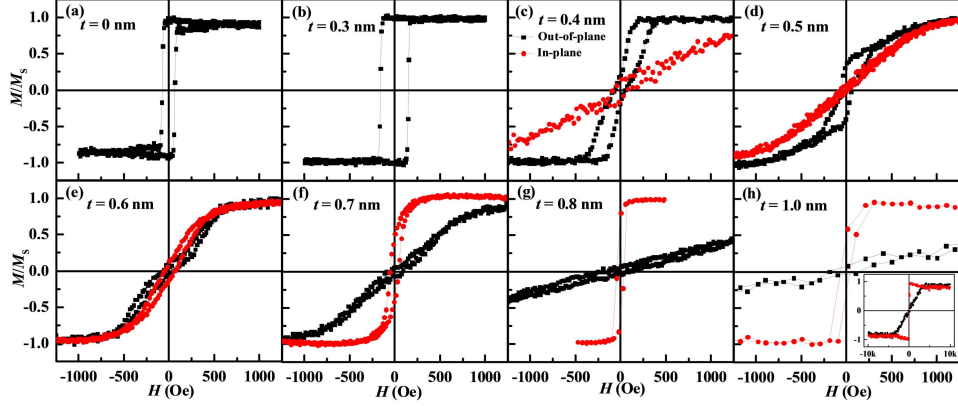


Fig. 1. OOP (■) and IP (●) hysteresis loops measured at room temperature of Ta (2 nm)/Pt (5 nm)/Co (1 nm)/CoFeB ( $t$  nm)/MgO (2 nm)/Ta (2 nm) thin films. The thickness of the CoFeB layers ( $t$ ) within the films is (a) 0 nm, (b) 0.3 nm, (c) 0.4 nm, (d) 0.5 nm, (e) 0.6 nm, (f) 0.7 nm, (g) 0.8 nm, and (h) 1.0 nm. The inset in (h) is  $M$ - $H$  loop of Ta (2 nm)/Pt (5 nm)/Co (1 nm)/CoFeB (1 nm)/MgO (2 nm)/Ta (2 nm) thin films up to 10 kOe.

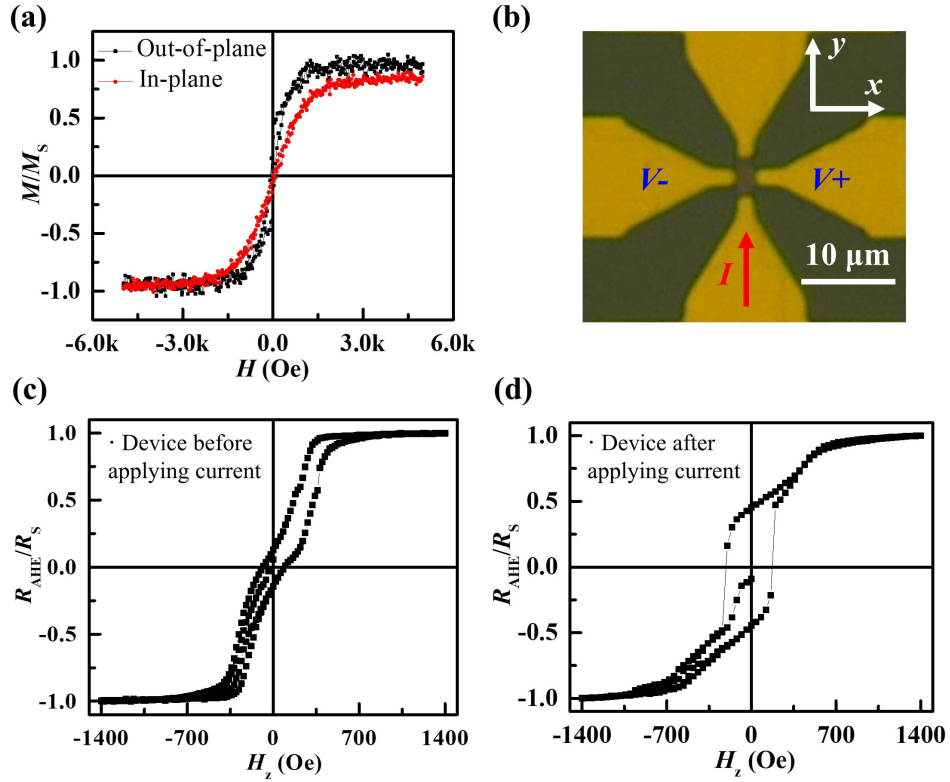


Fig. 2. (a) OOP and IP hysteresis loops from Ta 2/Pt 5/Co 1/CoFeB 0.45/MgO 2/Ta 2 (in nm) thin films. (b) Optical image of the Hall bar device made from the same film and the measurement configuration. Normalized anomalous Hall resistance ( $R_{\text{AHE}}/R_S$ ) curves as the function of the OOP applied magnetic field ( $H_z$ ) for the device (c) before and (d) after applying current.

in Fig. 1(a), with a square perpendicular hysteresis loop and high remanence ratio  $M_r/M_s$  (remanence magnetization/saturation magnetization) around 1. The anisotropy field, estimated as the field where the IP magnetization (hard-axis direction) and perpendicular magnetization curves merge, is larger than 10 kOe as the magnetization cannot be saturated in the IP direction by 10 kOe (not shown here). This high perpendicular anisotropy indicates the strong interface anisotropy of Pt/Co. The OPA is still maintained with  $t_{\text{CoFeB}}$  up to 0.3 nm, as shown in Fig. 1(b). However, the OPA is significantly reduced as  $t_{\text{CoFeB}}$  is further increased. As is clearly observable in Fig. 1(c)–(e), the OOP saturation field

dramatically increases with  $t_{\text{CoFeB}}$  and is accompanied by a corresponding decrease in OOP coercivity. Most importantly for the discussions here, the perpendicular remanence shows a clear decrease and its dominant IP-shaped anisotropy begins to significantly compete with the PMA of ESS stack when  $t_{\text{CoFeB}}$  is increased above 0.3 nm. It indicates that the moments of exchange spring magnet tilt toward the film plane, which is proved by the presence of an IP magnetization component, when further increase of the CoFeB thickness over 0.3 nm. IP remanence ratio increases on moving from the saturated state to 0.52, whereas the perpendicular ratio decreases to 0.06 when the CoFeB thickness increases up

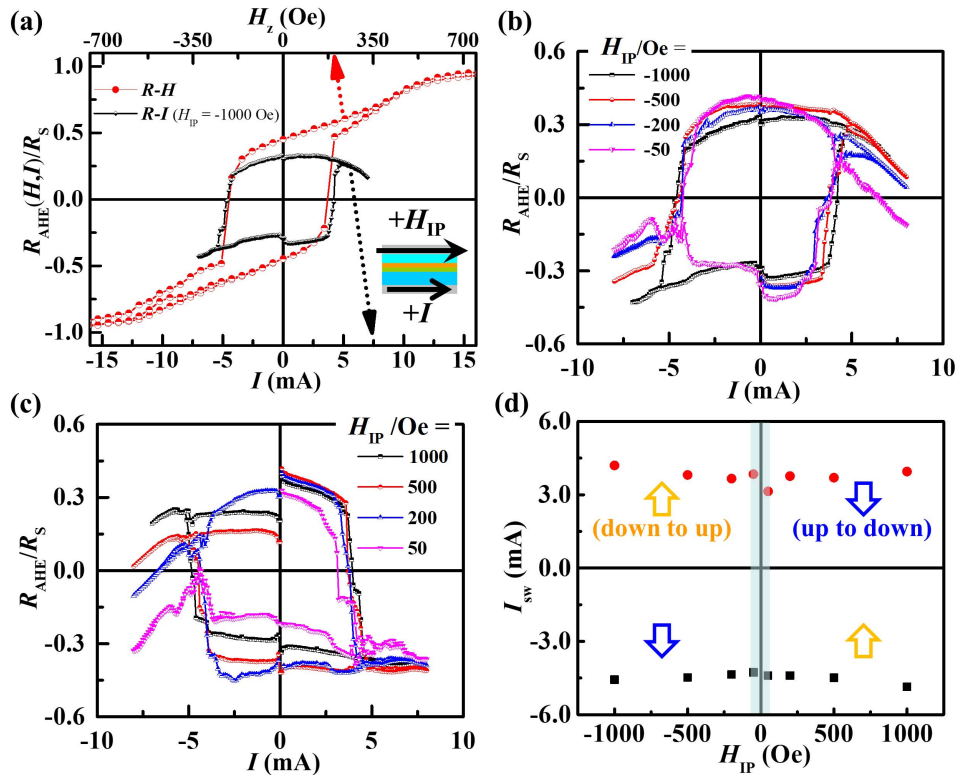


Fig. 3. Current-induced tilt magnetization switching in the device made from Ta 2/Pt 5/Co 1/CoFeB 0.45/MgO 2/Ta 2 (in nm) films. (a) Comparison of OOP field ( $H_z$ ) switching (red curve) with the current ( $I$ ) switching (black curve) in the presence of  $-1000$  Oe IP field ( $H_{\text{IP}}$ ), which is antiparallel to the current direction defined as in the inset. (b) Current-induced switching under negative  $H_{\text{IP}}$ . (c) Current-induced switching under positive  $H_{\text{IP}}$ , which is parallel to the current direction. (d) Phase diagram showing the switching current ( $I_{\text{sw}}$ ) as a function of  $H_{\text{IP}}$ .

to 0.7 nm, as illustrated in Fig. 1(f). The easy axis of ESS becomes totally IP when the CoFeB thickness is 0.8–1 nm, as depicted in Fig. 1(g) and (h). The magnetization tilt angle from OOP ( $\theta_M$ ) at remanence can be simply estimated using the following equation [4]:

$$\theta_M = \cos^{-1}(m_r/m_{r,\text{ref}}) \quad (1)$$

where  $m_r$  is the normalized remanence ( $M_r/M_S$ ) and  $m_{r,\text{ref}}$  is the reference remanence of the Co/Pt film without CoFeB, which shows a remanent magnetization pointing completely OOP for  $\theta_M = 0^\circ$ . As clearly shown in Fig. 1,  $\theta_M$  can be varied from 0 to  $90^\circ$  by simply varying  $t_{\text{CoFeB}}$ .

Fig. 2(a) shows the IP and OOP hysteresis loops for Ta 2/Pt 5/Co 1/CoFeB 0.45/MgO 2/Ta 2 (in nm) films, both IP and OOP coercivities are small compared to single Pt/Co films. The tilt angle from the OOP is estimated to be around  $45^\circ$  according to (1). The IP hysteresis loops were deviated from a linear shape, indicating that the amount of soft-magnetic phase CoFeB increased and the magnetization turns easily to the IP direction under an applied field. The reversed domain appeared in positive nucleation field at a positive saturation state and the magnetization of soft CoFeB was switched at this field ( $\sim 1.2$  kOe).

These films were then patterned into Hall bar structures with a channel width of  $2 \mu\text{m}$  and length of  $6 \mu\text{m}$  [Fig. 2(b)], using photolithography and ion milling techniques. Measurements of the dependence of the anomalous Hall effect (AHE) resistance ( $R_{\text{AHE}}$ ) on an OOP applied magnetic field ( $H_z$ ) were used to identify the equilibrium magnetization direction of the devices, as  $R_{\text{AHE}}$  is proportional to the perpendicular compo-

nent of magnetization ( $M_z$ ) in the ESS. The magnetization upward ( $M_z > 0$ ) and downward ( $M_z < 0$ ) corresponds to  $R_{\text{AHE}} > 0$  and  $R_{\text{AHE}} < 0$ , respectively. Here, the voltage generated by the AHE was measured along the  $x$ -axis and a current was applied along the  $y$ -axis. Fig. 2(c) shows the normalized AHE resistance  $R_{\text{AHE}}/R_s$  as a function of  $H_z$  under  $10 \mu\text{A}$  bias current for the device, where  $R_s$  is the saturation anomalous Hall resistance. As can be seen from the loop, the coercivity of the device ( $\sim 100$  Oe) is almost unchanged compared to that of the thin film. However, the coercivity significantly increases up to  $\sim 200\%$  after applying current (of  $8$  mA, here) on the device, as shown in Fig. 2(d). This enhancement in the coercivity may be due to the current-induced thermal effect.

For the SOT-driven magnetic switching measurement, a dc current ( $I$ ) was applied along the  $y$ -axis, and the anomalous Hall resistance  $R_{\text{AHE}}$  was recorded along the  $x$ -axis to monitor the change in the vertical component of the magnetization. A static magnetic field ( $H_{\text{IP}}$ ) was applied almost parallel (or antiparallel) to the IP current direction. The black curve of Fig. 3(a) shows the  $R-I$  loop in the presence of  $H_{\text{IP}} = -1000$  Oe. The sudden reversals and sharp jumps in  $R_{\text{AHE}}/R_s$  at  $I \sim \pm 4$  mA (the current density  $J \sim 2 \times 10^7 \text{ A/cm}^2$ ) are indicative of the current-induced magnetization switching. Moreover, the change of Hall resistance due to magnetization switching caused by the magnetic field and current is similar, as shown in Fig. 3(a). Fig. 3(b) and (c) shows the current-induced switching from up to down when  $I \cdot H_{\text{IP}} > 0$  and from down to up when  $I \cdot H_{\text{IP}} < 0$ , under either positive or negative  $H_{\text{IP}}$  of  $\pm 50$ ,  $\pm 200$ ,  $\pm 500$ ,

and  $\pm 1000$  Oe. The loops in Fig. 3(c) are not closed due to the temperature drift during measurements. It is interesting to note that the switching current magnitude ( $I_{sw}$ ) for the reversal in  $R_{AHE}$  or the magnetization in our ESS is almost independent of the  $H_{IP}$ , as shown in Fig. 3(d), which is consistent with the previous observation in Pt/Co/MgO [13] and Ta/CoFeB/MgO [14] structures. This might be explained by the magnetization switching induced by SOT and Dzyaloshinskii–Moriya interaction (DMI) under a  $H_{IP}$ , which occurs by the nucleation of the small reversed domains followed by the depinning and expansion of the reversed domains, as described in the following.

As shown in the red curve of Fig. 3(a), the  $R$ – $H$  loop shows a decrease from 1 to 0.3 in  $R_{AHE}/R_S$  for  $|H_z|$  smaller than the coercivity field, as attributed to the nucleation of reversed domains [15]. Similar to  $H_z$ , the effective field ( $H_{eff}$ ) generated by the current-induced SOT can also lead to the nucleation. Due to the presence of DMI in the Co/Pt interface [16], the domain walls (DWs) have a chirality with Néel type, for which  $H_{eff}$  acts on DWs for their motion but not the expansion of domains in the absence of  $H_{IP}$  because of the offset in vertical component of  $H_{eff}$  [17], that is, a deterministic SOT switching cannot be achieved at zero field. If  $H_{IP}$  is applied and is larger than the DMI effective field ( $H_{DMI}$ ) to break the DWs' chirality, the magnetic moments within the DWs are aligned parallel to the  $H_{IP}$ , as well as the current direction [18]. In this case,  $H_{eff}$  leads to the expansion of the reversed domains, consequently resulting in a full reversal. Furthermore, at  $H_{IP} > H_{DMI}$ , the ratio of the effective field and the current density ( $H_{eff}/J$ ) reaches the saturation and is independent of  $H_{IP}$  [14]. Therefore, once  $H_{IP} > H_{DMI}$ , the critical  $I_{sw}$ , required to provide a  $H_{eff}$  for the depinning and expansion of the reversed domains, will keep almost constant under different magnitudes of  $H_{IP}$ . Based on our ESS, we estimate  $H_{DMI} < 50$  Oe, which is smaller than that in the Co/Pt system without CoFeB soft layer ( $\sim 100$  Oe) [13]. Hence, a smaller  $H_{IP}$  can be used for SOT switching in ESS. In addition, at the same  $H_{IP}$  (e.g., 200 Oe), the critical switching current density in our ESS ( $\sim 2 \times 10^7$  A/cm $^2$ ) is reduced compared to that of the system with OOP only ( $\sim 4.5 \times 10^7$  A/cm $^2$  [13]).

#### IV. CONCLUSION

In summary, we explore the SOT switching of exchange coupled Pt/Co–CoFeB bilayers. We took the advantage of the competition between the IP-shaped anisotropy of the CoFeB and PMA of the Co/Pt, and then achieved the magnetization tilt angles from  $0^\circ$  to  $90^\circ$  by varying CoFeB's thickness from 0 to 1 nm, accordingly. IP current-induced magnetization switching of Co/Pt-CoFeB ESS is also investigated, under IP magnetic field with varied magnitudes. The switching current magnitude around  $2 \times 10^7$  A/cm $^2$  for the  $45^\circ$  tilt magnetization switching is almost independent of  $H_{IP}$  ranging from 50 to 1000 Oe. It indicates the DMI effective field of ESS may be less than 50 Oe, which is smaller than that of Co/Pt. This illuminates that the DMI in the chiral magnets might be tuned by exchange coupling. These results demonstrate the critical role of the IPA CoFeB layer in the current-induced

SOTs switching of exchange spring magnets and may help clarify the physics behinds SOTs in such ESS, especially in Co/Pt-CoFeB layers, which could be considered as a candidate system for future SOT-MRAM and SOT-oscillator devices.

#### ACKNOWLEDGMENT

The authors would like to thank Prof. S. Salahuddin from the University of California at Berkeley, Berkeley, CA, USA, for his help on this paper. This work was supported in part by the National Natural Science Foundation of China under Grant 61674062 and Grant 61821003 and in part by the Fundamental Research Funds for the Central Universities under Grant HUST: 2018KFYXKJC019. The work of O. Lee was supported by the KIST Institutional Program under Grant 2E29410.

#### REFERENCES

- [1] S. Mangin, D. Ravelosona, J. A. Katine, M. J. Carey, B. D. Terris, and E. E. Fullerton, "Current-induced magnetization reversal in nanopillars with perpendicular anisotropy," *Nature Mater.*, vol. 5, pp. 210–215, Feb. 2006.
- [2] X. Zhu and J.-G. Zhu, "Spin torque and field-driven perpendicular MRAM designs scalable to multi-Gb/chip capacity," *IEEE Trans. Magn.*, vol. 42, no. 10, pp. 2739–2741, Oct. 2006.
- [3] R. Sbiaa, R. Law, E.-L. Tan, and T. Liew, "Spin transfer switching enhancement in perpendicular anisotropy magnetic tunnel junctions with a canted in-plane spin polarizer," *J. Appl. Phys.*, vol. 105, Jan. 2009, Art. no. 013910.
- [4] S. Chung *et al.*, "Tunable spin configuration in [Co/Ni]-NiFe spring magnets," *J. Phys. D, Appl. Phys.*, vol. 46, Feb. 2013, Art. no. 125004.
- [5] J. P. Wang, Y. Y. Zou, C. H. Hee, T. C. Chong, and Y. F. Zheng, "Approaches to tilted magnetic recording for extremely high areal density," *IEEE Trans. Magn.*, vol. 39, no. 4, pp. 1930–1935, Jul. 2003.
- [6] M. Albrecht *et al.*, "Magnetic multilayers on nanospheres," *Nature Mater.*, vol. 4, pp. 203–206, Feb. 2005.
- [7] J.-P. Wang, "Magnetic data storage: Tilting for the top," *Nature Mater.*, vol. 4, no. 3, pp. 191–192, 2005.
- [8] D. Houssameddine *et al.*, "Spin-torque oscillator using a perpendicular polarizer and a planar free layer," *Nature Mater.*, vol. 6, pp. 447–453, Apr. 2007.
- [9] W. H. Rippard *et al.*, "Spin-transfer dynamics in spin valves with out-of-plane magnetized CoNi free layers," *Phys. Rev. B, Condens. Matter*, vol. 81, Jan. 2010, Art. no. 014426.
- [10] L. You *et al.*, "Switching of perpendicularly polarized nanomagnets with spin orbit torque without an external magnetic field by engineering a tilted anisotropy," *Proc. Nat. Acad. Sci. USA*, vol. 112, pp. 10310–10315, Aug. 2015.
- [11] Y. F. Zheng, J. P. Wang, and V. Ng, "Control of the tilted orientation of CoCrPt/Ti thin film media by collimated sputtering," *J. Appl. Phys.*, vol. 91, p. 8007, May 2002.
- [12] T. N. A. Nguyen *et al.*, "[Co/Pd]-NiFe exchange springs with tunable magnetization tilt angle," *Appl. Phys. Lett.*, vol. 98, Mar. 2011, Art. no. 172502.
- [13] O. J. Lee *et al.*, "Central role of domain wall depinning for perpendicular magnetization switching driven by spin torque from the spin Hall effect," *Phys. Rev. B, Condens. Matter*, vol. 89, Jan. 2014, Art. no. 024418.
- [14] J. Cao *et al.*, "Spin orbit torques induced magnetization reversal through asymmetric domain wall propagation in Ta/CoFeB/MgO structures," *Sci. Rep.*, vol. 8, Jan. 2018, Art. no. 1355.
- [15] C. Burrowes *et al.*, "Low depinning fields in Ta-CoFeB-MgO ultra-thin films with perpendicular magnetic anisotropy," *Appl. Phys. Lett.*, vol. 103, Oct. 2013, Art. no. 182401.
- [16] H. Yang, A. Thiaville, S. Rohart, A. Fert, and M. Chshiev, "Anatomy of Dzyaloshinskii–Moriya interaction at Co/Pt interfaces," *Phys. Rev. Lett.*, vol. 115, Dec. 2015, Art. no. 267210.
- [17] S. Emori, U. Bauer, S.-M. Ahn, E. Martinez, and G. S. D. Beach, "Current-driven dynamics of chiral ferromagnetic domain walls," *Nature Mater.*, vol. 12, pp. 611–616, Jun. 2013.
- [18] P. P. J. Haazen, E. Murè, J. H. Franken, R. Lavrijsen, H. J. M. Swagten, and B. Koopmans, "Domain wall depinning governed by the spin Hall effect," *Nature Mater.*, vol. 12, pp. 299–303, Feb. 2013.